5 May 1995

ELSEVIER

Chemical Physics Letters 237 (1995) 137–144

CHEMICAL PHYSICS LETTERS

A rigorous electrodynamic model for periodic structure formation during UV laser-induced metal atom deposition

Andrew C.R. Pipino, George C. Schatz, Richard P. Van Duyne

Department of Chemistry, Northwestern University, 2145 Sheridan Road, Evanston, IL 60208-3113, USA

Received 9 December 1994; in final form 27 February 1995

Abstract

A model is presented which describes the time and spatial frequency evolution of periodic structures formed during metal atom deposition arising from UV laser-induced photodissociation of organometallics. In addition to the occurrence of rapid growth of spatial frequencies which allow direct coupling of the incident radiation to the surface-plasmon polariton (SPP), a high-wavevector profile component, associated with the interference of counterpropagating SPP waves, also develops with extremely high gain but without feedback. Pump/probe diffraction methods for verifying the predictions and elucidating the surface modification of photodissociation are briefly proposed. Deposition of aluminum by photolysis of $(CH_3)_3Al$ at 257 nm is chosen as the model system.

1. Introduction

Laser-induced deposition of metal atoms by photodissociation of gas-phase and surface-adsorbed organometallic molecules has been an area of substantial activity in recent years [1]. Interest has been driven in part by applications where spatially resolved deposition of metal films is required, such as in the fabrication of microelectronic components [2]. These films are typically rough on the nanometer-length scale which can allow excitation of the surface-plasmon polariton (SPP) mode. Understanding the influence of a structured metal surface on photolysis of organometallics will allow optimization of the technology and provide fundamental insight into the surface modification of photochemistry.

Providing a dramatic example of surface-modified photochemistry, the spontaneous formation of periodic microstructures during metal atom deposition induced by UV laser photolysis of metal alkyls was first reported by Brueck and Ehrlich [3]. They observed the exponential growth of grating structures with mean groove spacings ranging from $\lambda/1.2$ to $\lambda/1.7$. Stimulated scattering of the incident radiation into the SPP mode was invoked to explain the phenomenon. To account for the occurrence of feedback, Brueck and Ehrlich obtained the small-signal gain for that spatial frequency which directly coupled the incident radiation into the SPP mode by using explicit expressions from perturbation theory. Jelski and George [4] extended this theoretical analysis by incorporating expressions for the surface fields which were expected to be valid at deep corrugations to estimate the limiting grating depth produced during deposition. Similar to theories for other surface-enhanced phenomena [5], both models assumed that the deposition rate at a point on the surface was proportional to the local intensity, which accounted at least semi-quantitatively for the observations. Indeed, from the surface-enhancement perspective, the

SSDI 0009-2614(95)00278-2

stimulated SPP scattering mechanism for spontaneous grating formation suggests a unique opportunity for the study of surface-modified photodissociation due to the deterministic morphology of grating structures. In particular, when combined with diffraction experiments, rigorous theories for describing the electrodynamics of corrugated surfaces potentially allow for a separation of molecule dependent and independent surface effects by providing an accurate description of the SPP-enhanced surface fields within a local dielectric constant approximation. Furthermore, diffraction measurements provide a real-time optical probe of the deposition process which responds only to changes in long-range order. By initiating the deposition on a seed grating, initial rates of SPP-enhanced deposition can be obtained under conditions where the surface fields are well characterized. In the case of photodissociation of metal alkyls, demonstration of spatial-frequency doubling [6] and the growth of spheroidal particles from spherical seed particles [7], attest to the feasibility of these experiments. Such studies could provide insight into the competition between surface enhancement of photodissociation and surface-induced relaxation of the relevant excited state [8], as well as useful kinetic data for these technologically important reactions [1]. The specific problem of photodissociation modified by a metallic diffraction grating has also been recently examined theoretically, using a point-dipole approximation for the molecule [9].

In this work, a simple but rigorous model describing the time and spatial frequency evolution of a metal film surface profile during UV laser-induced metal deposition is presented which should facilitate the design and interpretation of experiments related to SPP enhancement of photodissociation. The model is more rigorous than earlier models [3,4] in that the exact solution to Maxwell's equations within a local dielectric constant approximation is used to describe the surface fields. This approach allows the full interference structure of the surface intensity to affect profile growth. It is revealed that in addition to growth of spatial frequencies which couple the incident radiation directly to the SPP mode, the interference of counterpropagating SPP waves also induces deposition with high gain. The details of the model are discussed and calculations are presented for deposition of aluminum by photolysis of $(CH_3)_3Al$ at 257 nm. Some experimental strategies for measuring the influence of SPP-enhanced surface fields on deposition rates are then briefly described.

2. Theory

In the work of Brueck and Ehrlich [3] and of Jelski and George [4] only contributions from the interference between the incident radiation and one or two diffraction orders including the SPP-enhanced orders were included in the description of the surface intensity. A more general approach, which includes growth induced by higher-order SPP interactions, is obtained by Fourier transforming the full solution of Maxwell's equations for the electric field intensity in the vicinity of the surface. With the surface profile expressed as a general Fourier series, the rate law relating growth of the kth Fourier component of the surface to the kth Fourier component of the local intensity is then simply

$$\frac{d\zeta_k}{dt} = a(\omega, \theta_i) I_k, \tag{1}$$

where ζ_k is a cosine or sine amplitude, I_k is the corresponding field intensity amplitude, and $a(\omega, \theta_i)$ is a frequency and angle of incidence dependent proportionality constant. The surface fields can be obtained by using the extinction theorem method, but for weak corrugations the reduced Rayleigh equations offer a convenient solution.

The reduced Rayleigh equations for linear diffraction were originally developed by Toigo et al. [10]. Only the equations required for implementing the theory will be presented here. In the relevant geometry for SPP excitation, a p-polarized plane wave of frequency ω is incident from vacuum onto a corrugated metal surface described by the function $z = \zeta(x)$, with the plane of incidence taken to be perpendicular to the corrugations. As with any method based on the Rayleigh hypothesis, the reduced Rayleigh equations assume that Fourier expansions for the fields above and below the region of corrugation can be connected at the surface to satisfy the usual boundary conditions. Two infinite sets of coupled linear equations for the refracted and reflected amplitudes, including evanescent orders, are obtained. Using a simple transformation, the reflected

amplitudes are isolated and conveniently calculated from

$$\sum_p \frac{\beta_r \alpha_p + k_r k_p}{\beta_r - \alpha_p} Y_{r-p}(\beta_r, \alpha_p) A_p = \frac{\beta_r \alpha_0 - k_r k}{\beta_r + \alpha_0} Y_{r-0}(\beta_r, -\alpha_0), \quad (2)$$

with

$$Y_{r-p}(\beta_r, \alpha_r) = \frac{1}{a}\int_0^a \mathrm{d}x \exp\left(-\mathrm{i}\frac{2\pi}{a}(r-p)x - \mathrm{i}(\beta_r - \alpha_p)\zeta(x)\right) \quad (3)$$

and

$$\alpha_p(k|\omega) = \left[(\omega^2/c^2) - k_p^2\right]^{1/2}, \quad k_p^2 < \omega^2/c^2,$$
$$\alpha_p(k|\omega) = \mathrm{i}\left[k_p^2 - (\omega^2/c^2)\right]^{1/2}, \quad k_p^2 > \omega^2/c^2, \quad (4a)$$

$$\beta_p(k|\omega) = \left(\epsilon(\omega)\frac{\omega^2}{c^2} - k_p^2\right)^{1/2}, \quad \mathrm{Re}\,\beta_p > 0, \quad \mathrm{Im}\,\beta_p > 0, \quad (4b)$$

$$k_p = k + \frac{2\pi p}{a} = \frac{\omega}{c}\sin\theta + \frac{2\pi p}{a}, \quad p = 0, \pm 1, \pm 2, \ldots, \quad (4c)$$

where the complex dielectric function of the metal is given by $\epsilon(\omega)$. The amplitudes can be obtained from Eq. (2) by increasing the number of included diffraction orders until a preset convergence level is achieved. Given the magnetic field amplitudes, the electric field components are found from Faraday's law, and are given by

$$E_x(x, z) = \frac{1}{k_0}\left(-\alpha_0 \mathrm{e}^{\mathrm{i}kx - \mathrm{i}\alpha_0 z} + \sum_{-\infty}^{+\infty} \alpha_p A_p \mathrm{e}^{\mathrm{i}k_p x + \mathrm{i}\alpha_p z}\right), \quad (5a)$$

$$E_z(x, z) = \frac{1}{k_0}\left(-k\mathrm{e}^{\mathrm{i}kx - \mathrm{i}\alpha_0 z} - \sum_{-\infty}^{+\infty} k_p A_p \mathrm{e}^{\mathrm{i}k_p x + \mathrm{i}\alpha_p z}\right). \quad (5b)$$

Eqs. (5a) and (5b) describe the electric field rigorously for points above the region of corrugation, and are accurate for points within the selvedge region for weak corrugations in a properly converged calculation. Detailed discussions of the convergence properties of the reduced Rayleigh equations are available elsewhere [11]. For the deposition dynamics calculations, the surface fields are evaluated, somewhat arbitrarily, in the plane $z = \zeta_{\max}$, with the plane position being readjusted for each time step. Assuming randomly oriented precursor molecules, the growth rate obtained by this strategy will be simply proportional to the rate obtained by integrating over the decay length of the SPP. A more rigorous treatment should account for the modification of the excited state lifetime at short distances [9].

3. Results and discussion

The time evolution of two aluminum surfaces, obtained by integrating Eq. (1) for ten spatial harmonics, is shown in Figs. 1 and 2, which consider normal and oblique laser incidence, respectively. The proportionality constant in Eq. (1) is chosen to be wavevector independent and to provide growth rates which approximate experimental values. Aluminum deposition at 257 nm is modeled since this system has been extensively studied [12] and can provide clean deposition. In each figure, deposition is initiated on a low modulation seed grating which allows coupling to the SPP mode in a high order.

In Fig. 1, a 1% modulation grating with a 4862 Å period initially provides a second-order channel for SPP coupling at normal incidence. After a brief time period during which the seed grating amplitude decays, a second spatial harmonic is seen to emerge rapidly as anticipated in light of the results of Brueck and Ehrlich [3]. However, a fourth spatial harmonic also develops with comparable magnitude after a sufficient second harmonic amplitude has been established. In this case, deposition is induced by the interference of counterpropagating SPP waves – a result which only appears in an analysis which incorporates interactions beyond first order. Fig. 3 shows the small-signal-gain curves for the first five spatial harmonics obtained by Fourier transforming the surface field intensity after 5.5 s of deposition. Since

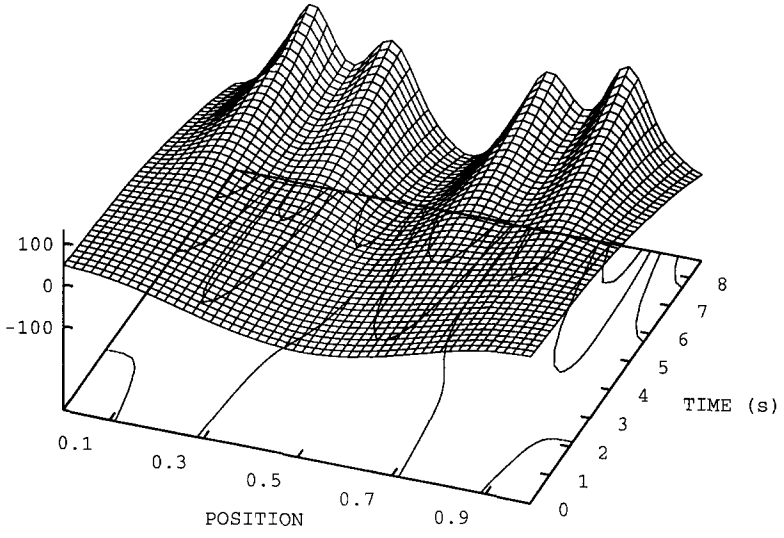

Fig. 1. The time evolution of an aluminum surface during Al atom deposition induced by photodissociation of $(CH_3)_3Al$ at 257 nm is modeled. A 4862 Å seed grating with an amplitude-to-period ratio of $\xi_0/a = 0.01$ initially provides second-order coupling to the doubly degenerate SPP mode at normal incidence. The integration time step is 0.01 s. Note the rapid development of both second and fourth spatial harmonics.

the fourth harmonic arises from the interference of two SPP-enhanced orders, gain for this component can be very large. However, because growth of the fourth harmonic is coupled to the second harmonic magnitude, feedback does not occur.

As originally reported [3], periodic microstructure growth can also be induced by an obliquely incident UV laser beam. Fig. 2 shows aluminum deposition on a 1% modulation, 9724 Å period seed grating which allows coupling to the SPP mode in third

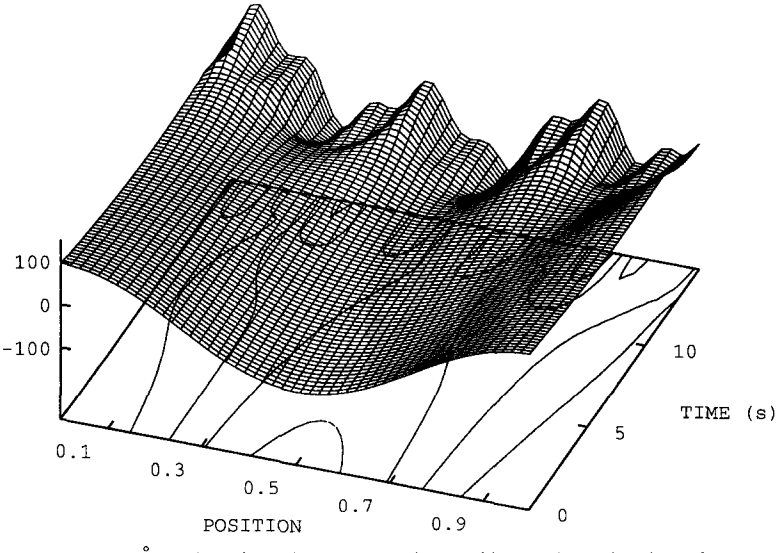

Fig. 2. Similar to Fig. 1, except a 9724 Å seed grating with $\xi_0/a = 0.01$ provides a third-order channel for SPP coupling. The third and eighth spatial harmonics are seen to emerge.

order at 257 nm. The angle of incidence was chosen at the preresonant angle of 14.65°. This angle maximizes gain for the spatial harmonic which directly couples the incident wave with the SPP by determining the phase of the SPP-enhanced field intensity with respect to the seed grating structure [6]. A distinct third harmonic is seen to initiate after approximately 10 s. An FFT analysis of the profile function reveals that the fifth harmonic which couples the incident radiation to the oppositely propagating SPP mode shows weak growth, while the eighth harmonic which arises from the interference of counterpropagating SPP waves grows in at a rate comparable to the third harmonic. As in the case of normal incidence, growth of the wavevector which couples the two branches of the SPP dispersion relation occurs through the interference of two SPP-enhanced, evanescent diffraction orders, although in the case of oblique incidence only one of these orders is strongly excited. Note that the wavevector of the profile component which arises from SPP–SPP interaction in both the normal and oblique incidence cases is essentially the same. Only the harmonic identity relative to the seed grating has changed between these two cases.

The use of a seed grating for initiating UV laser-induced deposition has been demonstrated as a method for growing phase-controlled, high wavevector gratings [6]. Seed gratings can be fabricated by holographic methods [13,14] which provide a high level of control over surface microstructure and therefore SPP coupling efficiency. The use of a seed grating also allows the convenience and simplicity of diffraction methods to be used to study the deposition process. For probing deposition induced by the interference of the incident radiation with an SPP-enhanced, evanescent order, simple first-order diffraction can be used under conditions where the probe frequency is high enough to provide a propagating first order. However, this limits the range of useful probe frequencies, since the most efficient growth of gratings by SPP coupling occurs for grating periods which are comparable to the incident wavelength. A strategy for circumventing this limitation is depicted in Fig. 4. By initiating the deposition on a seed grating with profile function $\zeta(x) = 0.01a(\sin kx + 0.5 \sin 3kx)$, which can be fabricated with reasonable precision by using Fourier blaze holography [14], both pump and probe beams can be coupled to SPP modes through separate profile components. The UV

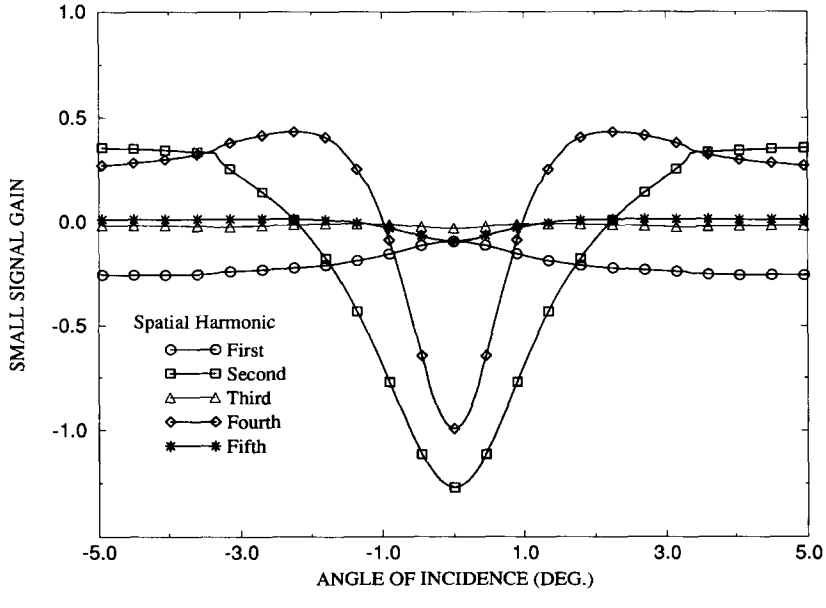

Fig. 3. The small-signal gain for the first five spatial harmonics after $t = 5.5$ s of deposition is plotted as a function of angle of incidence. Note the large gain for the inverted second and fourth spatial harmonics.

laser at ω_{pump} excites the SPP mode of the surface through the third spatial harmonic thereby creating an enhanced, periodic surface intensity which induces in-phase deposition for the proper choice of angle of incidence. The second laser excites the SPP mode at ω_{probe} through the fundamental component in the grating profile. Since the third spatial harmonic directly couples the SPP-enhanced, evanescent order at the probe frequency with the propagating -2 diffraction order, this order is especially sensitive to the deposition-induced profile changes. Small-signal gain calculations have been used to identify the seed grating profile which allows a simplified interpretation of the initial rate measurements. In the case considered, the magnitude of the seed profile third harmonic is initially chosen to be one-half the magnitude of the fundamental component, since this configuration happens to null the deposition-induced loss of the fundamental while gain for the third harmonic is large – inducing almost exclusive growth of this component in the profile. The probe beam then detects only growth of the component which feeds back to the SPP at the pump frequency. Therefore, by using the sensitivity of diffraction orders to spatial harmonics at the SPP coupling angle [15], the range of probe frequencies can be extended.

To probe the deposition induced by the interference of counterpropagating SPP waves, linear diffraction can also be used by choosing a frequency above the dissociation frequency to permit a propagating diffraction order which directly probes the profile component at $2k_{SPP}$. However, as shown in Fig. 5, growth of this very high wavevector profile component on a seed grating can also be probed by using *second harmonic diffraction* generated by a *visible* laser source. The case of deposition at normal incidence on a 4862 Å period seed grating with profile function $\zeta(x) = 0.01a(\cos kx + 0.5\cos 2kx)$ is depicted in Fig. 5. The incident probe frequency, ω_{probe}, is selected so that at $2\omega_{probe}$ a propagating -2 order exists when the SPP is excited in first order at ω_{probe}. This diffraction order is directly connected with the SPP-enhanced, evanescent $+2$ order by the fourth spatial harmonic. The -2 second harmonic order, calculated using the theory of Farias

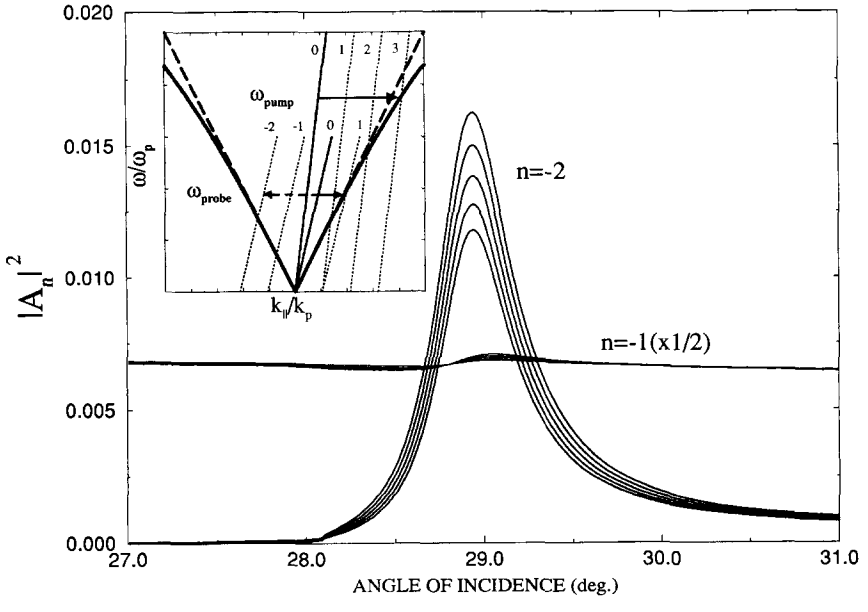

Fig. 4. A two laser linear diffraction technique is depicted for probing the deposition process. The nonspecular diffraction orders at $\omega_{probe} = 5145$ Å are shown for several time points during deposition. The time step is 0.1 s. Note that the -2 order is very sensitive to the deposition, while the other orders change negligibly. The ω–k diagram shows the SPP coupling details. Further explanation is provided in the text.

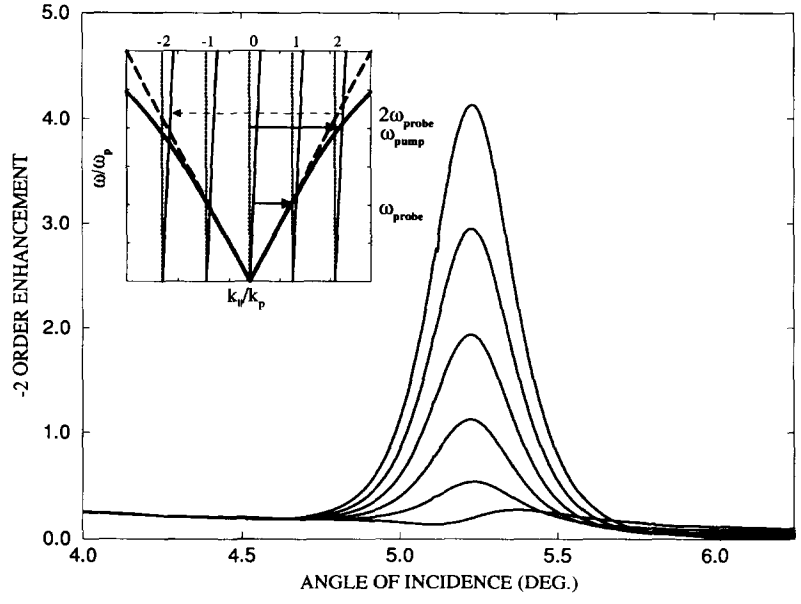

Fig. 5. A strategy for using second harmonic diffraction to probe deposition induced by the interference of counterpropagating SPP waves for a normally incident pump beam is demonstrated. The -2 second harmonic diffraction order is plotted for several time points during deposition. The time step is 0.01 s. The ω–k diagram shows how the existence of a propagating -2 second harmonic diffraction order provides a direct real time probe of the deposition-induced changes in the fourth spatial harmonic. Enhancement is defined relative to the corresponding flat surface response.

and Maradudin [16], is seen to increase rapidly during deposition as a result of the direct connection with the $+2$, SPP-enhanced order [17]. This method would provide a direct test of the deposition model.

4. Conclusions

Application of a rigorous electrodynamic theory to the problem of periodic structure formation during UV laser-induced metal atom deposition has demonstrated the importance of higher-order interactions in the growth process. Deposition induced by SPP–SPP interaction may account for the distribution in the mean groove spacing which has been observed experimentally [3]. However, perhaps more importantly, by combining a deposition dynamics model which is based on a rigorous diffraction theory with pump/probe diffraction experiments on seed gratings, a detailed understanding of the surface modification of photodissociation will likely be obtained. Small-signal-gain measurements on nanostructured gratings with well-characterized morphology and SPP coupling properties should allow elucidation of the competition between SPP enhancement of photolysis and surface-induced relaxation of the dissociative state. As originally predicted by Nitzan and Brus [8], this competition should result in an optimum molecule-to-surface distance for photolysis [9]. Wolkow and Moskovits [18] attempted to observe this competition by controlling the photoreactant-to-surface distance with adsorbed spacer layers on randomly rough silver surfaces. Although this strategy had been quite successfully applied to obtain the distance dependence of fluorescence on nominally flat metal surfaces, the strong dependence of the SPP-enhanced surface field on the presence of an overlayer and the random nature of the surface roughness, rendered their results essentially indecisive. In contrast, the surface fields on gratings are well-defined in the presence of an overlayer [19,20], which should allow the effect of surface-induced relaxation to be extracted.

Furthermore, in applications of laser-induced deposition, surface-localized photolysis is expected to provide greater spatial resolution in comparison to

gas-phase photolysis [1]. Yet a decisive strategy for distinguishing surface versus gas-phase photolysis has not been developed. In previous investigations [21–25], the beam diameter dependence of the deposition rate was used, but this has produced only ambiguous results. Since the SPP is relatively localized to the surface, with a decay length on the order of 100 nm, small-signal-gain measurements should also be useful for identifying conditions which favor surface versus gas-phase photolysis.

Acknowledgements

This work was supported in part by National Science Foundation grants CHE-940078 and CHE-9016490. We also thank the donors of the Petroleum Research Fund, grant 24134-AC6, administered by the American Chemical Society.

References

[1] I.P. Herman, Chem. Rev. 89 (1989) 1323.
[2] K.G. Ibbs and R.M. Osgood, eds., Laser chemical processing for microelectronics (Cambridge Univ. Press, Cambridge, 1989).
[3] S.R.J. Brueck and D.J. Ehrlich, Phys. Rev. Letters 48 (1982) 1678.
[4] D.A. Jelski and T.F. George, J. Appl. Phys. 61 (1987) 2353.
[5] M. Moskovits, Rev. Mod. Phys. 57 (1985) 783.
[6] D.J. Ehrlich and S.R.J. Brueck, Appl. Phys. Letters 47 (1985) 216.
[7] C.J. Chen and R.M. Osgood, Phys. Rev. Letters 50 (1983) 1705.
[8] A. Nitzan and L.E. Brus, J. Chem. Phys. 75 (1981) 2205.
[9] P.T. Leung and T.F. George, Phys. Rev. B 36 (1987) 4664.
[10] F. Toigo, A. Marvin, V. Celli and N.R. Hill, Phys. Rev. B 15 (1977) 5618.
[11] T.C. Paulick, Phys. Rev. B 42 (1990) 2801.
[12] K. Seki, J.M. Frye, H. Okabe and J.B. Halpern, J. Cryst. Growth 132 (1993) 25.
[13] S. Austin and F.T. Stone, Appl. Opt. 15 (1976) 1071.
[14] M. Breidne, S. Johansson, L.-E. Nilsson and H. Åhlèn, Opt. Acta 26 (1979) 1427.
[15] A.C.R. Pipino and G.C. Schatz, J. Opt. Soc. B 11 (1994) 2036.
[16] G.A. Farias and A.A. Maradudin, Phys. Rev. B 30 (1984) 3002.
[17] A.C.R. Pipino, G.C. Schatz and R.P. Van Duyne, Phys. Rev. B 49 (1994) 8320.
[18] R.A. Wolkow and M. Moskovits, J. Chem. Phys. 87 (1987) 5858.
[19] M. Arnold and K. Hehl, J. Mod. Opt. 40 (1993) 2423.
[20] M. Arnold, P. Bussemer, K. Hehl, H. Grabhorn and A. Otto, J. Mod. Opt. 39 (1992) 2329.
[21] T.H. Wood, J.C. White and B.A. Thacker, Appl. Phys. Letters 42 (1983) 408.
[22] C.J. Chen, J. Vacuum Sci. Technol. A 5 (1987) 3386.
[23] D. Braichotte and H.V.D. Bergh, Appl. Phys. A 45 (1988) 337.
[24] L. Konstantinov, R. Nowak and P. Hess, Appl. Phys. A 47 (1988) 171.
[25] K. Piglmayer and D. Bauerle, Appl. Phys. B 48 (1989) 453.